crystals

MDPI

Article

Eliminating Ambiguities in Electrical Measurements of Advanced Liquid Crystal Materials

Oleksandr V. Kovalchuk [1,2], Tetiana M. Kovalchuk [3] and Yuriy Garbovskiy [4,*]

[1] Institute of Physics, National Academy of Sciences of Ukraine, 03680 Kyiv, Ukraine; akoval@knutd.com.ua
[2] Department of Applied Physics and Higher Mathematics, Kyiv National University of Technologies and Design, 01011 Kyiv, Ukraine
[3] V. Lashkaryov Institute of Semiconductor Physics, National Academy of Sciences of Ukraine, 03680 Kyiv, Ukraine; tatnik1412@gmail.com
[4] Department of Physics and Engineering Physics, Central Connecticut State University, New Britain, CT 06050, USA
* Correspondence: ygarbovskiy@ccsu.edu

Abstract: Existing and future display and non-display applications of thermotropic liquid crystals rely on the development of new mesogenic materials. Electrical measurements of such materials determine their suitability for a specific application. In the case of molecular liquid crystals, their direct current (DC) electrical conductivity is caused by inorganic and/or organic ions typically present in small quantities even in highly purified materials. Important information about ions in liquid crystals can be obtained by measuring their DC electrical conductivity. Available experimental reports indicate that evaluation of the DC electrical conductivity of liquid crystals is a very non-trivial task as there are many ambiguities. In this paper, we discuss how to eliminate ambiguities in electrical measurements of liquid crystals by considering interactions between ions and substrates of a liquid crystal cell. In addition, we analyze factors affecting a proper evaluation of DC electrical conductivity of advanced multifunctional materials composed of liquid crystals and nanoparticles.

Keywords: liquid crystals; ions; nanomaterials; electrical measurements; electrical conductivity; ion generation

check for updates

Citation: Kovalchuk, O.V.; Kovalchuk, T.M.; Garbovskiy, Y. Eliminating Ambiguities in Electrical Measurements of Advanced Liquid Crystal Materials. *Crystals* **2023**, *13*, 1093. https://doi.org/10.3390/cryst13071093

Academic Editor: Ingo Dierking

Received: 27 June 2023
Revised: 7 July 2023
Accepted: 10 July 2023
Published: 13 July 2023

1. Introduction

Tunable liquid crystal components can be found in numerous devices and commercial products. They include ubiquitous liquid crystal displays [1–4], electrically controlled lenses [5,6], waveguides [7,8], waveplates and filters [9,10], spatial light modulators [11], diffractive elements [12,13], privacy windows and shutters [14–17], reconfigurable meta- and plasmonic devices [18–20], intensity modulators and lasers [21–23], sensors [24], and smart devices tailored to microwave and millimeter-wave applications [25–27]. As a rule, such devices rely on the reorientation of liquid crystals under the action of applied electric fields. This reorientation can be altered by ions typically present in molecular liquid crystals in minute quantities [28–31]. In the simplest case, a standard electric field screening effect caused by ions can result in unpredictable changes in the performance of liquid crystal devices [28–31]. In addition, ions in molecular liquid crystals can result in extra power losses due to the Joule heating effect. That's why electrical measurements of any new liquid crystal material are a standard part of its material characterization [32,33]. Last but not least, the presence of ions in liquid crystal materials is important for understanding the unusual behavior of ferroelectric nematic liquid crystals [34] and polymer stabilized liquid crystals [35,36].

The importance of properly performed electrical measurements of liquid crystals was emphasized in many papers [37,38]. Standard experimental techniques include dielectric and impedance spectroscopy [39–42], transient current measurements [43,44], residual

direct current (DC) voltage measurements [45,46], voltage holding ratio [45,47], and flicker minimization methods [47]. A proper evaluation of the DC electrical conductivity of liquid crystals is very critical because its value determines the suitability of mesogenic materials for a particular application [32,33]. In a typical experimental setting, the measurements of the electrical resistivity ρ_{LC} or its inverse, DC electrical conductivity $\lambda_{DC} = {}^{1}/_{\rho_{LC}}$, are routinely performed. As a rule, the DC electrical conductivity measurements of liquid crystals are carried out using a sandwich-type cell of a single thickness. Only a few papers report the values of the DC electrical conductivity and/or concentration of ions obtained for cells of several thicknesses [38,40,48–52]. Even though the process of measuring the ionic conductivity is rather straightforward, the reported values of the ionic conductivity even of the same type of liquid crystals (as an example, consider a standard nematic 5CB) can vary significantly (up to two orders of magnitude) depending on the cell thickness and time [31,40,49]. To reduce this ambiguity, in evaluating the values of the DC electrical conductivity of molecular liquid crystals it is important to consider interactions between ions and substrates of the liquid crystal cell. Such interactions can result in the time-dependent and thickness-dependent DC electrical conductivity of molecular liquid crystals [53–56]. Because systematic (i.e., combining experiment and modelling) studies of such ionic effects are still rather rare, it is both interesting and important to study them in greater detail.

Future liquid crystal technologies rely on the development of advanced liquid crystal materials. Mixing liquid crystals with nanomaterials is considered a promising way to produce such multifunctional materials [57–61]. From both academic and industrial points of view, it is crucial to study electrical properties of such materials. Research results obtained by independent teams during the last two decades point to very non-trivial ionic effects in liquid crystals doped with nanoparticles of different origins (ferroelectric [62–70], magnetic [52,71–78], semiconductor and dielectric [79–87], carbon-based [88–98], and metal [99–106], additional references can be found in recent topical reviews [31,107–109]). If nanoparticles are added to liquid crystals, an analysis of the existing literature also reveals a great variability of the reported values of ionic conductivity of seemingly similar materials making the comparison of the reported results a very difficult task [31,107–109]. As a result, a proper evaluation of the DC electrical conductivity of molecular liquid crystals doped with nanoparticles is quite a challenging problem because its value can be substantially affected by interactions between ions, nanomaterials, and substrates of a liquid crystal cell [53].

In this paper, we present an analysis of how interactions between ions, cell substrates, and nanoparticles can affect the value of the DC electrical conductivity of molecular liquid crystals in real experimental settings. We use already reported experimental results [38,50,52,54,110] and analyze them from the same conceptual approach with a hope that the presented analysis and suggestions would be useful for experimentalists measuring electrical properties of liquid crystal materials. By discussing several experimental cases in the framework of the Langmuir adsorption model, we point to the importance of the following experimentally observed outcomes of such interactions: (i) interactions between ions and substrates of a liquid crystal cell result in time dependence of the measured value of the DC electrical conductivity; (ii) the measured value of the DC electrical conductivity also depends on the cell thickness; (iii) under certain conditions, nanomaterials in molecular liquid crystals can behave as sources of ions and exhibit behavior similar to that of weak electrolytes. We also show that whenever nanoparticles are used to improve the functionality of liquid crystals, a proper electrical characterization of such advanced materials should consider the combined effect of interactions between ions, substrates, and nanoparticles. We also describe how to decouple these processes in a typical experimental setting. In addition, some suggestions to improve existing experimental procedures for the evaluation of the DC electrical conductivity of liquid crystal materials are provided.

2. Materials and Methods

The DC electrical conductivity was measured by applying a dielectric spectroscopy method [38,42,111]. Sandwich-type cells of known thickness were filled with nematic liquid crystals 5CB [54,110], MJ961180 [38,112], and 6CB [52]. Nematic liquid crystals 5CB were used to analyze the time-dependent electrical conductivity. The dependence of the DC electrical conductivity on the cell thickness was illustrated using nematic liquid crystals MJ961180, and the combined effects of the cell thickness and iron-oxide nanoparticles was studied in nematic liquid crystals 6CB. The cell thickness was controlled by means of spacers. Indium–tin oxide substrates were covered with polyimide thin films to impose either planar (5CB, MJ961180) or homeotropic (6CB) boundary conditions. Additional experimental details can be found in papers [38,52,110].

The DC electrical conductivity λ_{DC} was found by measuring the electrical conductivity λ_{AC} as a function of frequency f using an oscilloscopic technique (a version of impedance measurements when a known alternating current (AC) voltage signal V_{AC} of frequency f is applied across a sample, and the current through a sample I_{AC} is measured; in this case, V_{AC}, I_{AC}, and a phase lag between them are measured using an oscilloscope. This experimental setup allows us to perform the same type of electrical measurements as a standard impedance analyzer (Figure 1)). By knowing geometric parameters of the cell (its thickness and area), both dielectric permittivity and electrical conductivity can be found [111]. In the intermediate range of frequencies (~10^2–10^4 Hz), the dependence of the electrical conductivity on frequency can be approximated by a power law known as Jonscher's power law or the universal dielectric response:

$$\lambda_{AC} = \lambda_{DC} + Af^m \tag{1}$$

where A and m are empirical parameters [42,111].

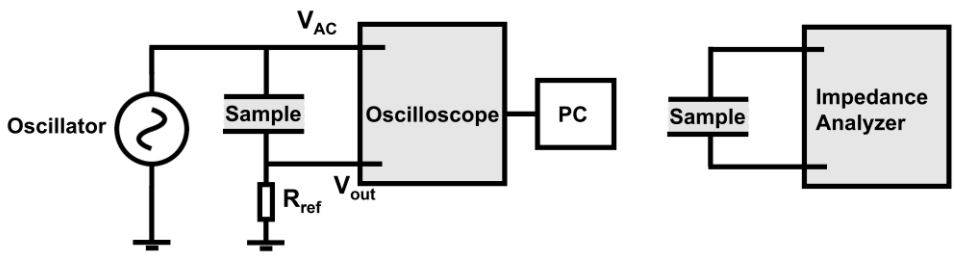

Figure 1. Schematic diagram of an experimental setup.

An analysis of the reported experimental results [38,52,110] was performed in the framework of the Langmuir adsorption model applied recently to molecular liquid crystals containing ions and nanoparticles [109]. An essential feature of this model is the consideration of the possibility of ionic contamination of the cell substrate and/or nanoparticles [109]. The details of this approach, its limitations, and its applicability to describe molecular liquid crystals with ions and nanomaterials can be found in recent papers [109,113].

3. Time-Dependent DC Electrical Conductivity of Liquid Crystal Cells

The first case study is related to the role of interactions between ions and substrates of the liquid crystal cell. In general, the liquid crystal substrates can act as a source of ions (if they are contaminated with ions) or they can capture ions already present in liquid crystals prior to filling an empty cell. In any real situation, we can expect a competition between ion-capturing and ion-releasing processes [113]. Experimental results reported in paper [110] allow us to analyze this competition between ionic processes in greater detail. According to [110], an empty cell was irradiated with a UV light prior to filling it with nematic liquid crystals 5CB. The source of UV light was a metal halide lamp (Panacol, Steinbach, Germany). The light intensity was 8 mW/cm^2. An ionizing UV light resulted in a generation of ions on the substrates of an empty liquid crystal cell. An empty cell exposed

to a UV light was filled with nematic liquid crystals 5CB and the DC electrical conductivity was measured as a function of time (Figure 2a, circles). The observed non-monotonous time dependence of the DC electrical conductivity can be explained in terms of the competition between ion-releasing and ion-capturing processes [54]. Some ions already present in liquid crystals (prior to filling an empty cell) are captured by the substrates of a liquid crystal cell (Figure 2b, black curve (n_1)). At the same time, ions present on the substrates of a liquid crystal cell can be released into the liquid crystal bulk (Figure 2b, red curve (n_2)). The combination of ion-releasing and ion-capturing processes, shown in Figure 2b, results in an experimentally observed non-monotonous dependence $\lambda_{DC}(t)$ (Figure 2a).

Solid curves, shown in Figure 2, can be generated by applying Equations (2)–(4), briefly discussed below (additional details can be found in paper [113]).

The DC electrical conductivity λ_{DC} of molecular liquid crystals is defined by Equation (2):

$$\lambda_{DC} = \sum_i q_i \mu_i n_i \tag{2}$$

where $q_i = |e| = 1.6 \times 10^{-19}$C ($i = 1,\ 2$), $n_i^+ = n_i^- = n_i$ is the volume concentration of ions of type i (we use index "1" ($i = 1$) to denote ions (fully dissociated ionic species) present in liquid crystals prior to filling an empty cell, and index "2" ($i = 2$) for ions generated by the substrates of a liquid crystal cell; $i = 1,\ 2$), and $\mu_i = \mu_i^+ + \mu_i^-$ is the effective ion mobility of ions of type i ($i = 1,\ 2$). Interactions between ions of type i and substrates are described by rate Equation (3):

$$\frac{dn_i}{dt} = -k_{Si}^{a\pm} n_i \frac{\sigma_{Si}}{d}\left(1 - \Theta_{S1}^{\pm} - \Theta_{S2}^{\pm}\right) + k_{Si}^{d\pm}\frac{\sigma_{Si}}{d}\Theta_{Si}^{\pm} \tag{3}$$

where the parameters $k_{Si}^{a\pm}$ and $k_{Si}^{d\pm}$ describe the time rate of ion-capturing and ion-releasing processes, respectively, and quantities $\Theta_{Si}^{\pm}$ stand for the fractional surface coverage of substrates by the i-th ions (i = 1, 2). Parameter σ_{Si} is the surface density of all surface sites on two substrates, and d is the cell thickness [113].

Equation (3) represents the conservation of the total number of ions of the i-th type:

$$n_{0i} + \frac{\sigma_{Si}}{d}\nu_{Si} = n_i + \frac{\sigma_{Si}}{d}\Theta_{\mathrm{Si}}^{\pm} \tag{4}$$

where n_{0i} is the initial concentration of ions of the i-th type in liquid crystals, and ν_{Si} is the contamination factor of substrates [113].

Table 1. Parameters used to generate solid curves shown in Figure 2.

Physical Parameter	Value
n_{01}	9.36×10^{20} m^{-3}
n_{02}	0 m^{-3}
σ_{S1}	1.6×10^{18} m^{-2}
σ_{S2}	1.6×10^{18} m^{-2}
$k_{S1}^{d\pm}$	3.5×10^{-4} s^{-1}
$k_{S2}^{d\pm}$	1×10^{-3} s^{-1}
$K_{S1} = k_{S1}^{a\pm}/k_{S1}^{d\pm}$	8.5×10^{-24} m^3
$K_{S2} = k_{S2}^{a\pm}/k_{S2}^{d\pm}$	7.37×10^{-24} m^3
ν_{S1}	0
ν_{S2}	6.325×10^{-3}
μ_1	1.92×10^{-10} m^2/Vs
μ_2	2.1×10^{-10} m^2/Vs
d	13.5 µm

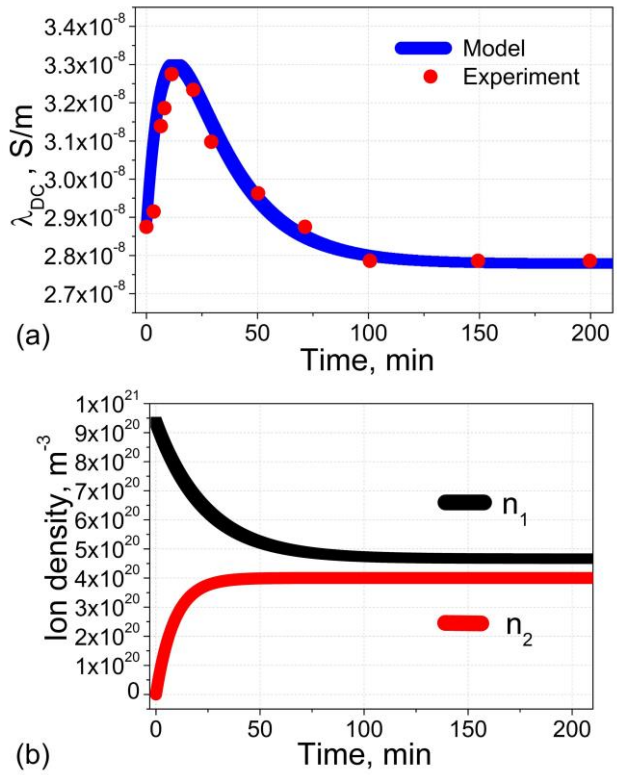

Figure 2. Time-dependent DC electrical conductivity and ion densities of nematic liquid crystals. The material parameters to generate solid curves are listed in Table 1. (**a**) Time-dependent DC electrical conductivity of a liquid crystal cell filled with nematic liquid crystals 5CB. The cell thickness is 13.5 µm. Red circles represent experimental datapoints reported in paper [110], and solid curve is a curve obtained by applying Equations (2)–(4). (**b**) The ion density of ions which were present in liquid crystals prior to filling an empty cell (n_1) and ions originated from the cell substrates (n_2) plotted as a function of time.

Solid curves, shown in Figure 2b, were generated by applying Equations (2)–(4) and using material parameters listed in Table 1. Figure 2b also reveals the presence of two characteristic time constants describing the ion-capturing ($\tau_1 = 23.7$ min) and ion-releasing ($\tau_2 = 8.9$ min) processes.

The results shown in Figure 2 suggest the adoption of the following experimental procedure for electrical measurements of liquid crystals. It is a good practice to record the time when an empty cell was filled with liquid crystals, and to measure the electrical conductivity as a function of time.

It should be noted that the model used to analyze the behavior of the DC electrical conductivity (Equations (2)–(4)) is elementary and has its limitations. Additional studies are required to uncover the mechanisms of ion generation in liquid crystal materials and liquid crystal substrates exposed to UV irradiation. Only a very limited number of publications can be found on this topic [114–116].

4. Steady-State DC Electrical Conductivity as a Function of the Cell Thickness

Equations (3) and (4) depend on the cell thickness. As a result, it can be expected that even a steady-state value of the DC electrical conductivity depends on the cell thickness. Indeed, the dependence of the DC electrical conductivity on the cell thickness was discussed in several papers [38,50]. Experimental results discussed in papers [38,50] were presented as a relative change in the DC electrical conductivity, $\Delta\lambda_{DC}/\lambda_{DC}$. Figure 3a shows an absolute value of the steady-state DC electrical conductivity of nematic liquid crystals MJ961190 plotted as a function of the cell thickness.

Table 2. Parameters used to generate solid curves shown in Figure 3.

Physical Parameter	Value
n_{01}	1.5×10^{19} m^{-3}
n_{02}	0 m^{-3}
σ_{S1}	3.6×10^{18} m^{-2}
σ_{S2}	0.75×10^{16} m^{-2}
$K_{S1} = k_{S1}^{a\pm}/k_{S1}^{d\pm}$	4.0×10^{-24} m^3
$K_{S2} = k_{S2}^{a\pm}/k_{S2}^{d\pm}$	5.0×10^{-24} m^3
ν_{S1}	0
ν_{S2}	2.5×10^{-2}
μ_1	2.5×10^{-9} m^2/Vs
μ_2	5.0×10^{-10} m^2/Vs

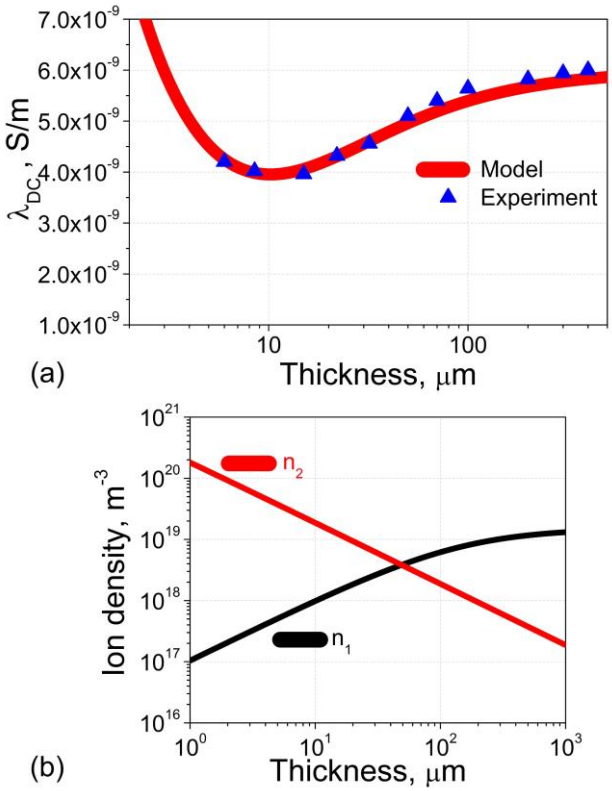

Figure 3. The dependence of the steady-state DC electrical conductivity and ion densities of nematic liquid crystals MJ961190 on the cell thickness. The material parameters to generate solid curves are listed in Table 2. (**a**) The dependence of the DC electrical conductivity of nematic liquid crystals MJ961190 on the cell thickness. (**b**) The dependence of the ion density of ions which were present in liquid crystals prior to filling an empty cell (n_1) and ions originated from the cell substrates (n_2) on the cell thickness.

The observed non-monotonous dependence $\lambda_{DC}(d)$ (Figure 3a) can be explained by considering the presence of two processes (ion capturing and ion releasing) modeled in Figure 3b. Ions present in liquid crystals prior to filling an empty cell (their ion density is n_1) are captured by the surface of the cell substrates. This ion-capturing effect becomes weaker (i.e., the concentration n_1 increases) as the cell gap increases (Figure 3b, black curve (n_1)). Once an empty cell is filled, ions originated from contaminated substrates are released into the bulk of liquid crystals. This ion-releasing effect is stronger in the case of thinner cells

and becomes weaker if thicker cells are used (in other words, the ion density n_2 decreases when the cell gap increases (Figure 3b, red curve (n_2))).

Solid curves, shown in Figure 3, were generated by solving Equations (2)–(4), assuming steady-state conditions ($dn_i/dt = 0$). Material parameters are listed in Table 2.

It should be stressed that the range of available experimental datapoints shown in Figure 3 is limited. The smallest cell thickness is 4 μm. Even though theoretical curves show the dependence of the electrical conductivity starting from the thickness of 1 μm, an elementary model used in this paper can reach its limits and may require some modifications in the case of very thin cells. In addition, for thicker cells (>100 μm), the quality of alignment can affect the measured values of electrical conductivity because of its anisotropy. Even though all studied samples were inspected under crossed polarizers to verify their planar alignment, the alignment quality of thicker cells gradually decreases with increases in the cell thickness.

Figure 3 allows us to suggest the following improvements to existing experimental procedures for evaluations of the DC electrical conductivity. Even in a steady-state regime, the value of the DC electrical conductivity should be measured using cells of several thicknesses to obtain an idea about possible ionic processes in such systems.

5. Steady-State DC Electrical Conductivity of Nematic Liquid Crystals 6CB Doped with Iron Oxide Nanoparticles

If nanoparticles are used to modify the properties of liquid crystals, the evaluation of the DC electrical conductivity becomes more challenging because ions can interact with both nanoparticles and substrates of the cell. Moreover, nanoparticles can also act as a source of ions due to their uncontrolled ionic contamination [117]. Under certain conditions, nanomaterials contaminated with ions can behave in molecular liquid crystals in a similar way as weak electrolytes do [117]. As a result, to obtain deeper insight into the origin of ionic processes in such systems, it is important to measure the DC electrical conductivity as a function of the concentration of nanoparticles and as a function of the cell thickness. While the former aspect of experimental research was addressed in many publications (references to original publications can be found in topical review [31]), the latter issue remains practically unexplored [52]. Therefore, it is interesting and instructive to apply the same Langmuir adsorption model to analyze recently reported experimental data obtained for nematic liquid crystals 6CB doped with iron oxide nanoparticles [52].

In this case, to account for nanoparticle-induced ionic processes, Equations (3) and (4) can be modified by adding new terms responsible for both ion capturing and ion releasing by nanoparticles (Equations (5) and (6)) [113]:

$$\frac{dn_i}{dt} = -k_{Si}^{a\pm} n_i \frac{\sigma_{Si}}{d}\left(1 - \Theta_{S1}^{\pm} - \Theta_{S2}^{\pm}\right) + k_{Si}^{d\pm}\frac{\sigma_{Si}}{d}\Theta_{Si}^{\pm} - k_{NPi}^{a\pm} n_i n_{NP} A_{NP}\sigma_{Si}^{NP}\left(1 - \Theta_{NP1}^{\pm} - \Theta_{NP2}^{\pm}\right) + k_{NPi}^{d\pm} n_{NP}\sigma_{Si}^{NP} A_{NP}\Theta_{NPi}^{\pm} \quad (5)$$

$$n_{0i} + \frac{\sigma_{Si}}{d}\nu_{Si} + n_{NP}A_{NP}\sigma_{Si}^{NP}\nu_{NPi} = n_i + \frac{\sigma_{Si}}{d}\Theta_{Si}^{\pm} + n_{NP}A_{NP}\sigma_{Si}^{NP}\Theta_{NPi}^{\pm} \quad (6)$$

where the subscript "*NP*" refers to nanoparticles, and A_{NP} is the surface area of a single nanoparticle.

Experimental datapoints and theoretical curves computed by applying Equations (2), (5), and (6) are shown in Figure 4. Figure 4 indicates that for a given cell thickness, measurements of the DC electrical conductivity as a function of the concentration of nanoparticles can reveal whether nanomaterials act as ion-capturing or ion-generating objects. In the case shown in Figure 4, nanoparticles behave as ion-generating objects. It should be noted that the ion-releasing effect becomes more pronounced for thicker cells (Figure 4, red curve (50 μm thick cell)) and weakens if thinner cells are used (Figure 4, black curve (5 μm thick cell)). This fact can be explained in the following way. The substrates of a liquid crystal cell can capture only a limited number of ions released by nanoparticles. As a result, as the cell thickness increases, the ion density of ions brought by contaminated nanoparticles into a

liquid crystal host also increases and leads to the increase in the electrical conductivity, as is evidenced from Figure 4.

Table 3. Parameters used to generate solid curves shown in Figures 4 and 5.

Physical Parameter	Value (5 μm Thick Cell)	Value (50 μm Thick Cell)
n_{01}	2.5×10^{20} m^{-3}	2.5×10^{20} m^{-3}
n_{02}	0 m^{-3}	0 m^{-3}
σ_{S1}	2.0×10^{18} m^{-2}	2.0×10^{18} m^{-2}
σ_{S2}	1.0×10^{18} m^{-2}	1.0×10^{18} m^{-2}
σ_{NP1}	2.0×10^{18} m^{-2}	2.0×10^{18} m^{-2}
σ_{NP2}	1.0×10^{18} m^{-2}	1.0×10^{18} m^{-2}
$K_{NP1} = k^{a\pm}_{NP1}/k^{d\pm}_{NP1}$	2.0×10^{-24} m^3	2.0×10^{-24} m^3
$K_{NP2} = k^{a\pm}_{NP2}/k^{d\pm}_{NP2}$	3.0×10^{-25} m^3	3.0×10^{-25} m^3
$K_{S1} = k^{a\pm}_{S1}/k^{d\pm}_{S1}$	1.0×10^{-24} m^3	1.0×10^{-24} m^3
$K_{S2} = k^{a\pm}_{S2}/k^{d\pm}_{S2}$	6.0×10^{-24} m^3	6.0×10^{-24} m^3
ν_{S1}	0	0
ν_{S2}	0	0
ν_{NP1}	0	0
ν_{NP2}	0.7×10^{-3}	3.2×10^{-3}
μ_1	6.32×10^{-10} m^2/Vs	6.32×10^{-10} m^2/Vs
μ_2	12.64×10^{-10} m^2/Vs	12.64×10^{-10} m^2/Vs
R_{NP}	2.5 nm	2.5 nm

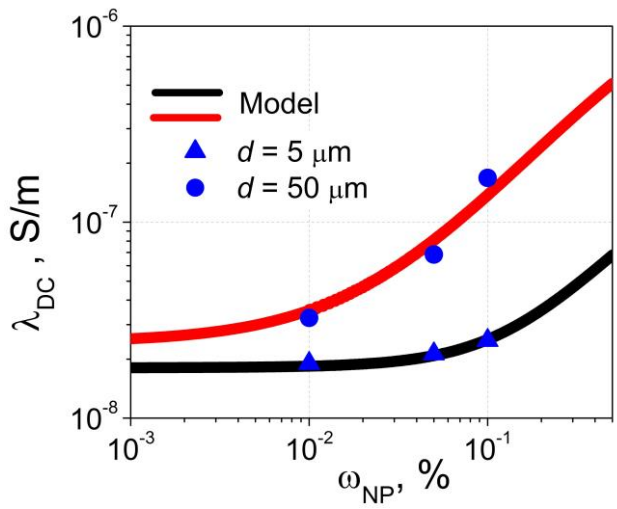

Figure 4. The dependence of the steady-state DC electrical conductivity of nematic liquid crystals 6CB on the weight concentration of iron oxide nanoparticles. The measurements were carried out using thin (5 μm) and thick (50 μm) cells. The material parameters to generate solid curves are listed in Table 3. Experimental datapoints are from paper [52].

Figure 5 offers additional insights into the ionic effects observed in liquid crystals 6CB doped with iron oxide nanoparticles. The concentration of ions which were present in liquid crystals prior to doping them with nanoparticles (n_1) decreases as the concentration of nanoparticles increases (Figure 5, black curves (n_1)). This is caused by the ion-capturing effect (nanoparticles capture ions). In addition, some fraction of such ions become trapped by the substrates of a cell. Figure 5a,b indicate that, in the case of ions which are inherently present in liquid crystals, the ion-capturing effect due to nanoparticles is much stronger than the ion-capturing effect due to the substrates for thicker cells (in this case, a noticeable

decrease in the ion density n_1 begins at lower values of the weight concentration of nanoparticles ω_{NP}). Figure 5 also shows that nanoparticles also act as a source of a new type of ions in liquid crystals (Figure 5, red curves (n_2)). The concentration of ions generated by nanoparticles (n_2) increases as the concentration of nanodopants increases (Figure 5, red curves (n_2)). Interestingly, this increase becomes weaker if thinner cells are used because ions released by contaminated nanoparticles become trapped by the surfaces of the liquid crystal cell. According to Figure 5, in the case of a 50 μm-thick cell the concentration of ions generated by nanoparticles is nearly one order of magnitude greater than that in the case of a 5 μm-thick cell.

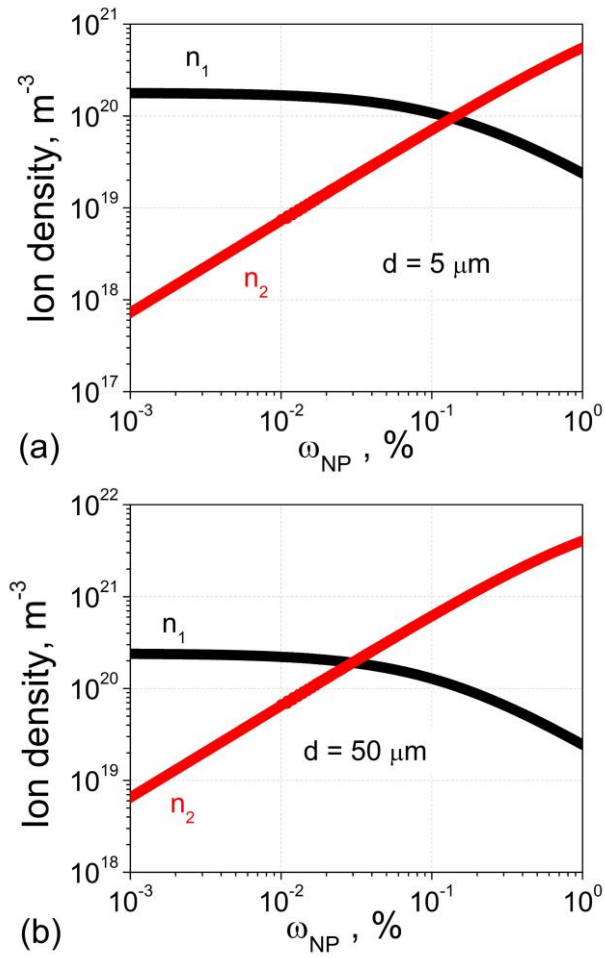

Figure 5. The dependence of the steady-state value of ion densities in nematic liquid crystals 6CB doped with iron oxide nanoparticles on the weight concentration of nanoparticles. The material parameters to generate solid curves are listed in Table 3. (**a**) The dependence of the ion density n_1 (ions which were present in liquid crystals prior to mixing them with nanoparticles) and of the ion density n_2 (ions originated in liquid crystals due to the ionic contamination of iron oxide nanoparticles) on the weight concentration of nanoparticles. The cell thickness is 5 μm (thin cell). (**b**) The dependence of the ion density n_1 (ions which were present in liquid crystals prior to mixing them with nanoparticles) and of the ion density n_2 (ions originated in liquid crystals due to the ionic contamination of iron oxide nanoparticles) on the weight concentration of nanoparticles. The cell thickness is 50 μm (thick cell).

It is interesting to comment on the values of material parameters used to generate solid curves shown in Figures 4 and 5. The values of all parameters listed in Table 3 are kept the same (for 5 μm and 50 μm thick cells) except for the value of the contamination factor of nanoparticles (its values it still on the order of 10^{-3} for both cases). Minor changes

in the preparation process of liquid crystals doped with nanoparticles can result in some changes in the level of ionic contamination of nanoparticles.

Figures 4 and 5 can be used for improving experimental procedures for assessing DC electrical conductivity of liquid crystals doped with nanoparticles. The ion-capturing and ion-releasing processes caused by interactions between ions, substrates, and nanoparticles can result in dependence of the DC electrical conductivity on the cell thickness and on the concentration of nanoparticles. The use of relatively thin cells can hinder the strength of nanoparticle-induced ion-capturing or ion-releasing effect. To reveal the effect of nanoparticles on the electrical conductivity of liquid crystals not affected by the substrates, thicker cells should be used.

6. Conclusions

The results presented in this paper have important practical implications. If an experimentalist is aimed at improving experimental procedures for evaluating the DC electrical conductivity of liquid crystal materials several factors should be considered. In the case of undoped liquid crystal materials, interactions between ions and substrates of a liquid crystal cell can results in time-dependent electrical conductivity (Figure 2). Moreover, the DC electrical conductivity also depends on the cell thickness even if a steady state is reached (Figure 3). Therefore, it is advisable to record the time when an empty cell is filled with liquid crystal materials and measure the electrical conductivity as a function of time until a steady state is reached. Such measurements can provide valuable information about ionic processes in liquid crystal materials and to what degree the DC electrical conductivity is affected by the cell substrates. Time-dependent experiments can also reveal whether the cell substrates act as a source of ion generation or a source of ion capturing. Additional insight into the ionic phenomena in liquid crystals can be obtained by measuring the dependence of the DC electrical conductivity on the cell thickness. Such measurements can identify a range of cell thicknesses corresponding to the situation when interactions between ions and cell substrates can alter the DC electrical conductivity of liquid crystals and the range of cell thicknesses which do not alter the DC electrical conductivity.

In the case of liquid crystals doped with nanomaterials, a proper evaluation of the DC electrical conductivity of such systems can be obtained by varying both the concentration of nanoparticles and the cell thickness (Figures 4 and 5). To understand the variations in the measured values of the DC electrical conductivity, interactions between ions, nanoparticles, and substrates of liquid crystal cells should be considered. It is important to realize the dual (both ion capturing and ion releasing) role played by the substrates and nanoparticles. The use of thin cells can hinder the effect of nanoparticles on the electrical conductivity of liquid crystals. To mitigate this effect, thicker cells can be used. At the same time, the alignment quality should also be considered because it can set a limit on the maximum value of the cell thickness.

An adoption of the proposed suggestions could help reduce or even eliminate ambiguities in electrical measurements of liquid crystal materials performed by independent research groups around the globe.

Author Contributions: Conceptualization, O.V.K. and Y.G.; methodology, O.V.K., T.M.K. and Y.G.; software, Y.G.; validation, O.V.K., T.M.K. and Y.G.; formal analysis, O.V.K., T.M.K. and Y.G.; investigation, O.V.K., T.M.K. and Y.G.; resources, O.V.K. and Y.G.; data curation, Y.G.; writing—original draft preparation, Y.G.; writing—review and editing, O.V.K., T.M.K. and Y.G.; visualization, O.V.K., T.M.K. and Y.G.; supervision, O.V.K. and Y.G.; project administration, Y.G.; funding acquisition, Y.G. All authors have read and agreed to the published version of the manuscript.

Funding: This research was funded by the 2023–2024 CSU—AAUP Faculty Research Grant and the NASA CT Space Grant.

Data Availability Statement: All data that support the findings of this study are included within the article.

Acknowledgments: The authors would like to acknowledge funding from the 2023–2024 CSU—AAUP Faculty Research Grant and the NASA CT Space Grant.

Conflicts of Interest: The authors declare no conflict of interest.

References

1. Koide, N. (Ed.). 50 years of liquid crystal R&D that lead the way to the future. In *The Liquid Crystal Display Story*; Springer: Tokyo, Japan, 2014.
2. Jones, C. The fiftieth anniversary of the liquid crystal display. *Liq. Cryst. Today* **2018**, *27*, 44–70. [CrossRef]
3. Xiong, J.; Hsiang, E.-L.; He, Z.; Zhan, T.; Wu, S.-T. Augmented reality and virtual reality displays: Emerging technologies and future perspectives. *Light Sci. Appl.* **2021**, *10*, 216. [CrossRef] [PubMed]
4. Wang, Y.-J.; Lin, Y.-H. Liquid crystal technology for vergence-accommodation conflicts in augmented reality and virtual reality systems: A review. *Liq. Cryst. Rev.* **2021**, *9*, 35–64. [CrossRef]
5. Algorri, J.F.; Zografopoulos, D.C.; Urruchi, V.; Sánchez-Pena, J.M. Recent Advances in Adaptive Liquid Crystal Lenses. *Crystals* **2019**, *9*, 272. [CrossRef]
6. Lin, Y.; Wang, Y.; Reshetnyak, V. Liquid crystal lenses with tunable focal length. *Liq. Cryst. Rev.* **2017**, *5*, 111–143. [CrossRef]
7. d'Alessandro, A.; Asquini, R. Light Propagation in Confined Nematic Liquid Crystals and Device Applications. *Appl. Sci.* **2021**, *11*, 8713. [CrossRef]
8. Shin, Y.; Jiang, Y.; Wang, Q.; Zhou, Z.; Qin, G.; Yang, D.K. Flexoelectric-effect-based light waveguide liquid crystal display for transparent display. *Photon. Res.* **2022**, *10*, 407–414. [CrossRef]
9. Abdulhalim, I. Non-display bio-optic applications of liquid crystals. *Liq. Cryst. Today* **2011**, *20*, 44–60. [CrossRef]
10. Chigrinov, V.G. *Liquid Crystal Photonics*; Nova Science Pub Inc.: New York, NY, USA, 2014; 204p.
11. Otón, J.M.; Otón, E.; Quintana, X.; Geday, M.A. Liquid-crystal phase-only devices. *J. Mol. Liq.* **2018**, *267*, 469–483. [CrossRef]
12. De Sio, L.; Roberts, D.E.; Liao, Z.; Hwang, J.; Tabiryan, N.; Steeves, D.M.; Kimball, B.R. Beam shaping diffractive wave plates. *Appl. Opt.* **2018**, *57*, A118–A121. [CrossRef]
13. Morris, R.; Jones, C.; Nagaraj, M. Liquid Crystal Devices for Beam Steering Applications. *Micromachines* **2021**, *12*, 247. [CrossRef]
14. Geis, M.W.; Bos, P.J.; Liberman, V.; Rothschild, M. Broadband optical switch based on liquid crystal dynamic scattering. *Opt. Express* **2016**, *24*, 13812–13823. [CrossRef] [PubMed]
15. He, Z.; Zeng, J.; Zhu, S.; Zhang, D.; Ma, C.; Zhang, C.; Yu, P.; Miao, Z. A bistable light shutter based on polymer stabilized cholesteric liquid crystals. *Opt. Mater.* **2023**, *136*, 113426. [CrossRef]
16. Sung, G.-F.; Wu, P.-C.; Zyryanov, V.Y.; Lee, W. Electrically active and thermally passive liquid-crystal device toward smart glass. *Photon Res.* **2021**, *9*, 2288–2295. [CrossRef]
17. Luo, L.; Liang, Y.; Feng, Y.; Mo, D.; Zhang, Y.; Chen, J. Recent Progress on Preparation Strategies of Liquid Crystal Smart Windows. *Crystals* **2022**, *12*, 1426. [CrossRef]
18. Liu, S.; Xu, F.; Zhan, J.; Qiang, J.; Xie, Q.; Yang, L.; Deng, S.; Zhang, Y. Terahertz liquid crystal programmable metasurface based on resonance switching. *Opt. Lett.* **2022**, *47*, 1891–1894. [CrossRef] [PubMed]
19. Chen, W.T.; Zhu, A.Y.; Capasso, F. Flat optics with dispersion-engineered metasurfaces. *Nat. Rev. Mater.* **2020**, *5*, 604–620. [CrossRef]
20. Jeng, S.C. Applications of Tamm plasmon-liquid crystal devices. *Liq. Cryst.* **2020**, *47*, 1223–1231. [CrossRef]
21. Chiang, W.; Silalahi, H.; Chiang, Y.C.; Hsu, M.C.; Zhang, Y.S.; Liu, J.H.; Yu, Y.; Lee, C.R.; Huang, C.Y. Continuously tunable intensity modulators with large switching contrasts using liquid crystal elastomer films that are deposited with terahertz metamaterials. *Opt. Express* **2020**, *28*, 27676–27687. [CrossRef]
22. Pozhidaev, E.P.; Minchenko, M.V.; Kuznetsov, A.V.; Tkachenko, T.P.; Barbashov, V.A. Broad temperature range ferrielectric liquid crystal as a highly sensitive quadratic electro-optical material. *Opt. Lett.* **2022**, *47*, 1598–1601. [CrossRef]
23. Lu, H.; Shi, J.; Wang, Q.; Xue, Y.; Yang, L.; Xu, M.; Zhu, J.; Qiu, L.; Ding, Y.; Zhang, J. Tunable multi-mode laser based on robust cholesteric liquid crystal microdroplet. *Opt. Lett.* **2021**, *46*, 5067–5070. [CrossRef]
24. Schenning, A.P.H.J.; Crawford, G.P.; Broer, D.J. (Eds.). *Liquid Crystal Sensors*; CRC Press, Taylor & Francis Group: Boca Raton, FL, USA, 2018; 164p.
25. Camley, R.; Celinski, Z.; Garbovskiy, Y.; Glushchenko, A. Liquid crystals for signal processing applications in the microwave and millimeter wave frequency ranges. *Liq. Cryst. Rev.* **2018**, *6*, 17–52. [CrossRef]
26. Jakoby, R.; Gaebler, A.; Weickhmann, C. Microwave Liquid Crystal Enabling Technology for Electronically Steerable Antennas in SATCOM and 5G Millimeter-Wave Systems. *Crystals* **2020**, *10*, 514. [CrossRef]
27. Ma, J.; Choi, J.; Park, S.; Kong, I.; Kim, D.; Lee, C.; Youn, Y.; Hwang, M.; Oh, S.; Hong, W.; et al. Liquid Crystals for Advanced Smart Devices with Microwave and Millimeter-Wave Applications: Recent Progress for Next-generation Communications. *Adv. Mater.* 2023, 2302474, *accepted author manuscript*. [CrossRef]
28. Blinov, L.M. *Structure and Properties of Liquid Crystals*; Springer: New York, NY, USA, 2010.
29. Neyts, K.; Beunis, F. Ion Transport in Liquid Crystals. In *Handbook of Liquid Crystals: Physical Properties and Phase Behavior of Liquid Crystals*; Wiley-VCH: Weinheim, Germany, 2014; Volume 2, Chapter 11; pp. 357–382.

30. Éber, N.; Salamon, P.; Buka, Á. Electrically induced patterns in nematics and how to avoid them. *Liq. Cryst. Rev.* **2016**, *4*, 101–134. [CrossRef]
31. Garbovskiy, Y. Conventional and unconventional ionic phenomena in tunable soft materials made of liquid crystals and nanoparticles. *Nano Express* **2021**, *2*, 012004. [CrossRef]
32. Naemura, S. Electrical properties of liquid crystal materials for display applications. *Mater. Res. Soc. Symp. Proc.* **1999**, *559*, 263–274. [CrossRef]
33. Goodby, J.W.; Cowling, S.J. Conception, Discovery, Invention, Serendipity and Consortia: Cyanobiphenyls and Beyond. *Crystals* **2022**, *12*, 825. [CrossRef]
34. Kumari, P.; Basnet, B.; Wang, H.; Lavrentovich, O.D. Ferroelectric nematic liquids with conics. *Nat. Commun.* **2023**, *14*, 748. [CrossRef] [PubMed]
35. Lee, K.M.; Bunning, T.J.; White, T.J.; McConney, M.E.; Godman, N.P. Effect of Ion Concentration on the Electro-Optic Response in Polymer-Stabilized Cholesteric Liquid Crystals. *Crystals* **2021**, *11*, 7. [CrossRef]
36. Lee, K.M.; Marsh, Z.M.; Crenshaw, E.P.; Tohgha, U.N.; Ambulo, C.P.; Wolf, S.M.; Carothers, K.J.; Limburg, H.N.; McConney, M.E.; Godman, N.P. Recent Advances in Electro-Optic Response of Polymer-Stabilized Cholesteric Liquid Crystals. *Materials* **2023**, *16*, 2248. [CrossRef]
37. Colpaert, C.; Maximus, B.; Meyere, D. Adequate measuring techniques for ions in liquid crystal layers. *Liq. Cryst.* **1996**, *21*, 133–142. [CrossRef]
38. Kovalchuk, O.V.; Glushchenko, A.; Garbovskiy, Y. Improving experimental procedures for assessing electrical properties of advanced liquid crystal materials. *Liq. Cryst.* **2023**, *50*, 140. [CrossRef]
39. Barbero, G.; Evangelista, L.R. *Adsorption Phenomena and Anchoring Energy in Nematic Liquid Crystals*; Taylor & Francis: Boca Raton, FL, USA, 2006.
40. Khazimullin, M.V.; Lebedev, Y.A. Influence of dielectric layers on estimates of diffusion coefficients and concentrations of ions from impedance spectroscopy. *Phys. Rev. E* **2019**, *100*, 062601. [CrossRef] [PubMed]
41. Karaawi, A.R.; Gavrilyak, M.V.; Boronin, V.A.; Gavrilyak, A.M.; Kazachonok, J.V.; Podgornov, F.V. Direct current electric conductivity of ferroelectric liquid crystals–gold nanoparticles dispersion measured with capacitive current technique. *Liq. Cryst.* **2020**, *47*, 1507–1515. [CrossRef]
42. Barrera, A.; Binet, C.; Dubois, F.; Hébert, P.-A.; Supiot, P.; Foissac, C.; Maschke, U. Temperature and frequency dependence on dielectric permittivity and electrical conductivity of recycled Liquid Crystals. *J. Mol. Liq.* **2023**, *378*, 121572. [CrossRef]
43. Vaxiviere, J.; Labroo, B.; Martinot-Lagarde, P. Ion Bump in the Ferroelectric Liquid Crystal Domains Reversal Current. *Mol. Cryst. Liq. Cryst. Inc. Nonlinear Opt.* **1989**, *173*, 61–73. [CrossRef]
44. Sugimura, A.; Matsui, N.; Takahashi, Y.; Sonomura, H.; Naito, H.; Okuda, M. Transient currents in nematic liquid crystals. *Phys. Rev. B* **1991**, *43*, 8272–8276. [CrossRef] [PubMed]
45. Inoue, M. Review of various measurement methodologies of migration ion influence on LCD image quality and new measurement proposal beyond LCD materials. *J. Soc. Inf. Disp.* **2020**, *28*, 92–110. [CrossRef]
46. Mizusaki, M.; Ishihara, S. A Novel Technique for Determination of Residual Direct-Current Voltage of Liquid Crystal Cells with Vertical and In-Plane Electric Fields. *Symmetry* **2021**, *13*, 816. [CrossRef]
47. Sasaki, N. A new measurement method for ion density in TFT-LCD panels. *Mol. Cryst. Liq. Cryst. Sci. Technol. Sect. A Mol. Cryst. Liq. Cryst.* **2001**, *367*, 671–679. [CrossRef]
48. Dhara, S.; Madhusudana, N.V. Ionic contribution to the dielectric properties of a nematic liquid crystal in thin cells. *J. Appl. Phys.* **2001**, *90*, 3483–3488. [CrossRef]
49. Kumar, A.; Varshney, D.; Prakash, J. Role of ionic contribution in dielectric behaviour of a nematic liquid crystal with variable cell thickness. *J. Mol. Liq.* **2020**, *303*, 112520. [CrossRef]
50. Kovalchuk, O.V. Adsorption of ions and thickness dependence of conductivity in liquid crystal. *Semicond. Phys. Quantum Electron. Optoelectron.* **2011**, *14*, 452–455. [CrossRef]
51. Shukla, R.K.; Chaudhary, A.; Bubnov, A.; Raina, K.K. Multiwalled carbon nanotubes-ferroelectric liquid crystal nanocomposites: Effect of cell thickness and dopant concentration on electro-optic and dielectric behaviour. *Liq. Cryst.* **2018**, *45*, 1672–1681. [CrossRef]
52. Kovalchuk, O.; Kovalchuk, T.; Tomašovičová, N.; Timko, M.; Zakutanska, K.; Miakota, D.; Kopčanský, P.; Shevchuk, O.; Garbovskiy, Y. Dielectric and electrical properties of nematic liquid crystals 6CB doped with iron oxide nanoparticles. The combined effect of nanodopant concentration and cell thickness. *J. Mol. Liq.* **2022**, *366*, 120305. [CrossRef]
53. Garbovskiy, Y. Ions and size effects in nanoparticle/liquid crystal colloids sandwiched between two substrates. The Case of Two Types Fully Ionized Species. *Chem. Phys. Lett.* **2017**, *679*, 77–85. [CrossRef]
54. Garbovskiy, Y. Time-dependent electrical properties of liquid crystal cells: Unravelling the origin of ion generation. *Liq. Cryst.* **2018**, *45*, 1540–1548. [CrossRef]
55. Webb, D.; Garbovskiy, Y. Overlooked Ionic Phenomena Affecting the Electrical Conductivity of Liquid Crystals. *Eng. Proc.* **2021**, *11*, 1. [CrossRef]
56. Webb, D.; Garbovskiy, Y. Steady-State and Transient Electrical Properties of Liquid Crystal Cells. *Chem. Proc.* **2022**, *9*, 15. [CrossRef]

57. Lagerwall, J.P.F.; Scalia, G. (Eds.). *Liquid Crystals with Nano and Microparticles*; World Scientific: Singapore, 2016; Volume 2; ISBN 978-981-4619-25-7.
58. Shen, Y.; Dierking, I. Perspectives in Liquid-Crystal-Aided Nanotechnology and Nanoscience. *Appl. Sci.* **2019**, *9*, 2512. [CrossRef]
59. Dierking, I. Nanomaterials in Liquid Crystals. *Nanomaterials* **2018**, *8*, 453. [CrossRef] [PubMed]
60. Lee, W.; Kumar, S. *Unconventional Liquid Crystals and Their Applications*; De Gruyter: Berlin, Germany; Boston, MA, USA, 2021.
61. Rastogi, A.; Mishra, A.; Pandey, F.P.; Manohar, R.; Parmar, A.S. Enhancing physical characteristics of thermotropic nematic liquid crystals by dispersing in various nanoparticles and their potential applications. *Emergent Mater.* **2023**, *6*, 101. [CrossRef]
62. Shukla, R.K.; Liebig, C.M.; Evans, D.R.; Haase, W. Electro-optical behaviour and dielectric dynamics of harvested ferroelectric $LiNbO_3$ nanoparticle-doped ferroelectric liquid crystal nanocolloids. *RSC Adv.* **2014**, *4*, 18529–18536. [CrossRef]
63. Basu, R.; Garvey, A. Effects of ferroelectric nanoparticles on ion transport in a liquid crystal. *Appl. Phys. Lett.* **2014**, *105*, 151905. [CrossRef]
64. Hsiao, Y.G.; Huang, S.M.; Yeh, E.R.; Lee, W. Temperature-dependent electrical and dielectric properties of nematic liquid crystals doped with ferroelectric particles. *Displays* **2016**, *44*, 61–65. [CrossRef]
65. Al-Zangana, S.; Turner, M.; Dierking, I. A comparison between size dependent paraelectric and ferroelectric $BaTiO_3$ nanoparticle doped nematic and ferroelectric liquid crystals. *J. Appl. Phys.* **2017**, *121*, 085105. [CrossRef]
66. Kumar, P.; Debnath, S.; Rao, N.V.S.; Sinha, A. Nanodoping: A route for enhancing electro-optic performance of bent core nematic system. *J. Phys. Condens. Matter.* **2018**, *30*, 095101. [CrossRef]
67. Shoarinejad, S.; Mohammadi Siahboomi, R. Ordering behavior and electric response of a ferroelectric nano-doped liquid crystal with ion impurity effects. *J. Appl. Phys.* **2021**, *129*, 025101. [CrossRef]
68. Lalik, S.; Deptuch, A.; Jaworska-Gołab, T.; Fryń, P.; Dardas, D.; Stefańczyk, O.; Urbańska, M.; Marzec, M. Modification of AFLC Physical Properties by Doping with $BaTiO_3$ Particles. *J. Phys. Chem. B* **2020**, *124*, 6055. [CrossRef] [PubMed]
69. Łoś, J.; Drozd-Rzoska, A.; Rzoska, S.J. Critical-like behavior of low-frequency dielectric properties in compressed liquid crystalline octyloxycyanobiphenyl (8OCB) and its nanocolloid with paraelectric $BaTiO_3$. *J. Mol. Liq.* **2023**, *377*, 121555. [CrossRef]
70. Salah, M.B.; Nasri, R.; Alharbi, A.N.; Althagafi, T.M.; Soltani, T. Thermotropic liquid crystal doped with ferroelectric nanoparticles: Electrical behavior and ion trapping phenomenon. *J. Mol. Liq.* **2022**, *357*, 119142. [CrossRef]
71. Mertelj, A.; Lisjak, D. Ferromagnetic nematic liquid crystals. *Liq. Cryst. Rev.* **2017**, *5*, 1–33. [CrossRef]
72. Studenyak, I.P.; Kopčanský, P.; Timko, M.; Mitroova, Z.; Kovalchuk, O.V. Effects of non-additive conductivity variation for a nematic liquid crystal caused by magnetite and carbon nanotubes at various scales. *Liq. Cryst.* **2017**, *44*, 1709. [CrossRef]
73. Gao, L.; Dai, Y.; Li, T.; Tang, Z.; Zhao, X.; Li, Z.; Meng, X.; He, Z.; Li, J.; Cai, M.; et al. Enhancement of Image Quality in LCD by Doping γ-Fe_2O_3 Nanoparticles and Reducing Friction Torque Difference. *Nanomaterials* **2018**, *8*, 911. [CrossRef]
74. Jessy, P.J.; Radha, R.; Patel, N. Highly improved dielectric behaviour of ferronematic nanocomposite for display application. *Liq. Cryst.* **2019**, *46*, 772.
75. Dalir, N.; Javadian, S. Evolution of morphology and electrochemical properties of colloidal nematic liquid crystal doped with carbon nanotubes and magnetite. *J. Mol. Liq.* **2019**, *287*, 110927. [CrossRef]
76. Meng, X.; Li, J.; Lin, Y.; Liu, X.; Liu, N.; Ye, W.; Li, D.; He, Z. Polymer dispersed liquid crystals doped with low concentration γ-Fe_2O_3 nanoparticles. *Liq. Cryst.* **2021**, *48*, 1791. [CrossRef]
77. Meng, X.; Li, J.; Lin, Y.; Liu, X.; Li, G.; Zhao, J.; Miao, Y.; Li, W.; Ye, W.; Li, D.; et al. Electro-optical response of polymer-dispersed liquid crystals doped with γ-Fe_2O_3 nanoparticles. *Liq. Cryst.* **2022**, *49*, 855. [CrossRef]
78. Meng, X.; Li, J.; Lin, Y.; Liu, X.; Zhao, J.; Li, D.; He, Z. Optimization approach for the dilute magnetic polymer-dispersed liquid crystal. *Opt. Mater.* **2022**, *131*, 112670. [CrossRef]
79. Shcherbinin, D.; Konshina, E. Ionic impurities in nematic liquid crystal doped with quantum dots CdSe/ZnS. *Liq. Cryst.* **2017**, *44*, 648. [CrossRef]
80. Shcherbinin, D.P.; Konshina, E.A. Impact of titanium dioxide nanoparticles on purification and contamination of nematic liquid crystals. *Beilstein J. Nanotechnol.* **2017**, *8*, 2766–2770. [CrossRef]
81. Yadav, G.; Katiyar, R.; Pathak, G.; Manohar, R. Effect of ion trapping behavior of TiO_2 nanoparticles on different parameters of weakly polar nematic liquid crystal. *J. Theor. Appl. Phys.* **2018**, *12*, 191. [CrossRef]
82. Konshina, E.; Shcherbinin, D.; Kurochkina, M. Comparison of the properties of nematic liquid crystals doped with TiO_2 and CdSe/ZnS nanoparticles. *J. Mol. Liq.* **2018**, *267*, 308–314. [CrossRef]
83. Rastogi, A.; Agrahari, K.; Pathak, G.; Srivastava, A.; Herman, J.; Manohar, R. Study of an interesting physical mechanism of memory effect in nematic liquid crystal dispersed with quantum dots. *Liq. Cryst.* **2019**, *46*, 725. [CrossRef]
84. Prakash, J.; Khan, S.; Chauhan, S.; Biradar, A. Metal oxide-nanoparticles and liquid crystal composites: A review of recent progress. *J. Mol. Liq.* **2020**, *297*, 112052. [CrossRef]
85. Seidalilir, Z.; Soheyli, E.; Sabaeian, M.; Sahraei, R. Enhanced electrochemical and electro-optical properties of nematic liquid crystal doped with Ni:ZnCdS/ZnS core/shell quantum dots. *J. Mol. Liq.* **2020**, *320*, 114373. [CrossRef]
86. Rani, A.; Chakraborty, S.; Sinha, A. Effect of CdSe/ZnS quantum dots doping on the ion transport behavior in nematic liquid crystal. *J. Mol. Liq.* **2021**, *342*, 117327. [CrossRef]
87. Chauhan, G.; Malik, P.; Deep, A. Morphological, dielectric, electro-optic and photoluminescence properties of titanium oxide nanoparticles enriched polymer stabilized cholesteric liquid crystal composites. *J. Mol. Liq.* **2023**, *376*, 121406. [CrossRef]

88. Lisetski, L.; Minenko, S.; Samoilov, A.; Lebovka, N. Optical density and microstructure-related properties of photoactive nematic and cholesteric liquid crystal colloids with carbon nanotubes. *J. Mol. Liq.* **2017**, *235*, 90. [CrossRef]
89. Tomylko, S.; Yaroshchuk, O.; Koval'chuk, O.; Lebovka, N. Structural evolution and dielectric properties of suspensions of carbon nanotubes in nematic liquid crystals. *Phys. Chem. Chem. Phys.* **2017**, *19*, 16456. [CrossRef] [PubMed]
90. Basu, R.; Lee, A. Ion trapping by the graphene electrode in a graphene-ITO hybrid liquid crystal cell. *Appl. Phys. Lett.* **2017**, *111*, 161905. [CrossRef]
91. Cetinkaya, M.; Yildiz, S.; Ozbek, H. The effect of -COOH functionalized carbon nanotube doping on electro-optical, thermo-optical and elastic properties of a highly polar smectic liquid crystal. *J. Mol. Liq.* **2018**, *272*, 801. [CrossRef]
92. Shukla, R.K.; Chaudhary, A.; Bubnov, A.; Hamplova, V.; Raina, K.K. Electrically switchable birefringent self-assembled nanocomposites: Ferroelectric liquid crystal doped with the multiwall carbon nanotubes. *Liq. Cryst.* **2020**, *47*, 1379. [CrossRef]
93. Barrera, A.; Binet, C.; Dubois, F.; Hébert, P.-A.; Supiot, P.; Foissac, C.; Maschke, U. Dielectric Spectroscopy Analysis of Liquid Crystals Recovered from End-of-Life Liquid Crystal Displays. *Molecules* **2021**, *26*, 2873. [CrossRef] [PubMed]
94. Barrera, A.; Binet, C.; Dubois, F.; Hébert, P.-A.; Supiot, P.; Foissac, C.; Maschke, U. Recycling of liquid crystals from e-waste. *Detritus* **2022**, *55*, 55–61. [CrossRef]
95. Kumar Singh, P.; Dubey, P.; Dhar, R.; Dabrowski, R. Functionalized and non-functionalized multi walled carbon nanotubes in the anisotropic media of liquid crystalline material. *J. Mol. Liq.* **2023**, *369*, 120889. [CrossRef]
96. Chausov, D.; Kurilov, A.; Smirnova, A.; Stolbov, D.; Kucherov, R.; Emelyanenko, A.; Savilov, S.; Usol'tseva, N. Mesomorphism, dielectric permittivity, and ionic conductivity of cholesterol tridecylate doped with few-layer graphite fragments. *J. Mol. Liq.* **2023**, *374*, 121139. [CrossRef]
97. Shivaraja, S.; Sahai, M.; Gupta, R.; Manjuladevi, V. Superior electro-optical switching properties in polymer dispersed liquid crystals prepared with functionalized carbon nanotube nanocomposites of LC for switchable window applications. *Opt. Mater.* **2023**, *137*, 113546. [CrossRef]
98. Lisetski, L.; Bulavin, L.; Lebovka, N. Effects of Dispersed Carbon Nanotubes and Emerging Supramolecular Structures on Phase Transitions in Liquid Crystals: Physico-Chemical Aspects. *Liquids* **2023**, *3*, 246–277. [CrossRef]
99. Middha, M.; Kumar, R.; Raina, K. Photoluminescence tuning and electro-optical memory in chiral nematic liquid crystals doped with silver nanoparticles. *Liq. Cryst.* **2016**, *43*, 1002. [CrossRef]
100. Podgornov, F.V.; Wipf, R.; Stühn, B.; Ryzhkova, A.V.; Haase, W. Low-frequency relaxation modes in ferroelectric liquid crystal/gold nanoparticle dispersion: Impact of nanoparticle shape. *Liq. Cryst.* **2016**, *43*, 1536. [CrossRef]
101. Urbanski, M.; Lagerwall, J.P.F. Why organically functionalized nanoparticles increase the electrical conductivity of nematic liquid crystal dispersions. *J. Mater. Chem. C* **2017**, *5*, 8802. [CrossRef]
102. Yan, X.; Zhou, Y.; Liu, W.; Liu, S.; Hu, X.; Zhao, W.; Zhou, G.; Yuan, D. Effects of silver nanoparticle doping on the electro-optical properties of polymer stabilized liquid crystal devices. *Liq. Cryst.* **2020**, *47*, 1131. [CrossRef]
103. Shivaraja, S.J.; Gupta, R.K.; Kumar, S.; Manjuladevi, V. Enhanced electro-optical response of nematic liquid crystal doped with functionalised silver nanoparticles in twisted nematic configuration. *Liq. Cryst.* **2020**, *47*, 1678.
104. Chausov, D.N.; Kurilov, A.D.; Kucherov, R.N.; Simakin, A.V.; Gudkov, S.V. Electro-optical performance of nematic liquid crystals doped with gold nanoparticles. *J. Phys. Condens. Matter* **2020**, *32*, 395102. [CrossRef]
105. Debnath, A.; Mandal, P.K.; Sarma, A.; Gutowski, O. Effect of silver nanoparticle doping on the physicochemical properties of a room temperature ferroelectric liquid crystal mixture. *J. Mol. Liq.* **2020**, *319*, 114185. [CrossRef]
106. Basu, R.; Gess, D.T. Ion trapping, reduced rotational viscosity, and accelerated electro-optic response characteristics in gold nano-urchin–nematic suspensions. *Phys. Rev. E* **2023**, *107*, 024705. [CrossRef]
107. Garbovskiy, Y. Nanomaterials in Liquid Crystals as Ion-Generating and Ion-Capturing Objects. *Crystals* **2018**, *8*, 264. [CrossRef]
108. Garbovskiy, Y. Nanoparticle—Enabled Ion Trapping and Ion Generation in Liquid Crystals. *Adv. Condens. Matter Phys.* **2018**, *2018*, 8914891. [CrossRef]
109. Garbovskiy, Y. A perspective on the Langmuir adsorption model applied to molecular liquid crystals containing ions and nanoparticles. *Front. Soft Matter.* **2022**, *2*, 1079063. [CrossRef]
110. Kravchuk, R.; Koval'chuk, O.; Yaroshchuk, O. Filling initiated processes in liquid crystal cell. *Mol. Cryst. Liq. Cryst.* **2002**, *384*, 111–119. [CrossRef]
111. Barsoukov, E.; Macdonald, J.R. *Impedance Spectroscopy: Theory, Experiment, and Applications*, 2nd ed.; Wiley-Interscience: Hoboken, NJ, USA, 2005.
112. Yaroshchuk, O.V.; Kiselev, A.D.; Kravchuk, R.M. Liquid-crystal anchoring transitions on aligning substrates processed by a plasma beam. *Phys. Rev. E* **2008**, *77*, 031706. [CrossRef] [PubMed]
113. Garbovskiy, Y. Kinetics of Ion-Capturing/Ion-Releasing Processes in Liquid Crystal Devices Utilizing Contaminated Nanoparticles and Alignment Films. *Nanomaterials* **2018**, *8*, 59. [CrossRef] [PubMed]
114. Lackner, A.M.; Margerum, J.D.; Van Ast, C. Near ultraviolet photostability of liquid crystal mixtures. *Mol. Cryst. Liq. Cryst.* **1986**, *141*, 289–310. [CrossRef]
115. Xu, H.; Davey, A.B.; Wilkinson, T.D.; Crossland, W.A.; Chapman, J.; Duffy, W.L.; Kelly, S.M. Performance of UV-stable STN Mixtures for PL-LCDs. *Mol. Cryst. Liq. Cryst.* **2004**, *411*, 79–91. [CrossRef]

116. Konovalov, V.; Fauchille, J.; Yakovenko, S. A lifetime model for LCOS panel under intense illumination. *J. SID* **2006**, *14*, 247–256. [CrossRef]
117. Garbovskiy, Y. On the Analogy between Electrolytes and Ion-Generating Nanomaterials in Liquid Crystals. *Nanomaterials* **2020**, *10*, 403. [CrossRef]